

Detecting and Modeling Earthquake Swarms in the Salton Trough, California

2010 NEHRP Grant G10AP00004

Final Report

Jeffrey McGuire,
Department of Geology and Geophysics, MS24
Woods Hole Oceanographic Institution
Woods Hole MA 02543

Abstract

Aseismic deformation transients such as fluid flow, magma migration, and slow slip can trigger changes in seismicity rate. We present a method that can detect these seismicity rate variations and utilize these anomalies to constrain the underlying variations in stressing rate. Because ordinary aftershock sequences often obscure changes in the background seismicity caused by aseismic processes, we combine the stochastic Epidemic Type Aftershock Sequence model that describes aftershock sequences well and the physically based rate- and state-dependent friction seismicity model into a single seismicity rate model that models both aftershock activity and changes in background seismicity rate. We implement this model into a data assimilation algorithm that inverts seismicity catalogs to estimate space-time variations in stressing rate. We evaluate the method using a synthetic catalog, and then apply it to a catalog of $M \geq 1.5$ events that occurred in the Salton Trough from 1990-2009. We validate our stressing rate estimates by comparing them to estimates from a geodetically-derived slip model for a large creep event on the Obsidian Buttes fault. The results demonstrate that our approach can identify large aseismic deformation transients in a multi-decade long earthquake catalog and roughly constrain the absolute magnitude of the stressing rate transients. Our method can therefore provide a way to detect aseismic transients in regions where geodetic resolution in space or time is poor.

Report:

2010 Primary Accomplishments

1. This grant funded the final year of Andrea Llenos' PhD thesis in the MIT-WHOI joint program. She graduated in 2010 and started a Post-doctoral fellowship at Stanford University. In 2011 she moved on to a Mendenhall Post-doctoral fellowship at the U.S.G.S. Earthquake Hazard's program in Menlo Park CA, supervised by Jeanne Hardebeck and Andy Michael.
2. In 2010 we submitted the primary technique development and data analysis paper from this project to the Journal of Geophysical Research. This paper,

- “Detecting Aseismic Strain Transients from Seismicity Data” by Llenos and McGuire, has been accepted by JGR and should be published in spring 2011.
3. The primary scientific accomplishments related to NEHRP objectives are the demonstration in the above paper (and see below) that our stochastic seismicity analysis algorithm can estimate the magnitude of stress-rate transients in southern California. This result was benchmarked using geodetic data and swarms from the Obsidian Buttes area of the Salton Trough.

Summary of Results

We applied our algorithm to earthquake data from the Salton Trough in southern California [Figure 1]. In the Salton Trough, a transition occurs from a divergent plate boundary setting in the Gulf of California to the south, to the San Andreas strike-slip fault system to the north. The region is characterized by high heat flow [*Kisslinger and Jones, 1991*], which potentially acts to subdue aftershock activity [*Ben-Zion and Lyakhovsky, 2006; Yang and Ben-Zion, 2009; Enescu et al., 2009*]. A high rate of earthquake swarm activity has been observed [e.g., *Richter, 1958; Brune and Allen, 1967; Hill et al., 1975; Johnson and Hadley, 1976; Lohman and McGuire, 2007; Roland and McGuire, 2009*], possibly driven by magmatic intrusion [*Hill, 1977*] or aseismic fault creep [*Lohman and McGuire, 2007; Roland and McGuire, 2009*]. Geodetic measurements have also detected a number of aseismic transients in this region, including afterslip following the 1987 M6.6 Superstition Hills earthquake [*Williams and Magistrale, 1989*], creep events on the Superstition Hills fault [*Wei et al., 2009*], and aseismic creep on the Obsidian Buttes fault [*Lohman and McGuire, 2007*].

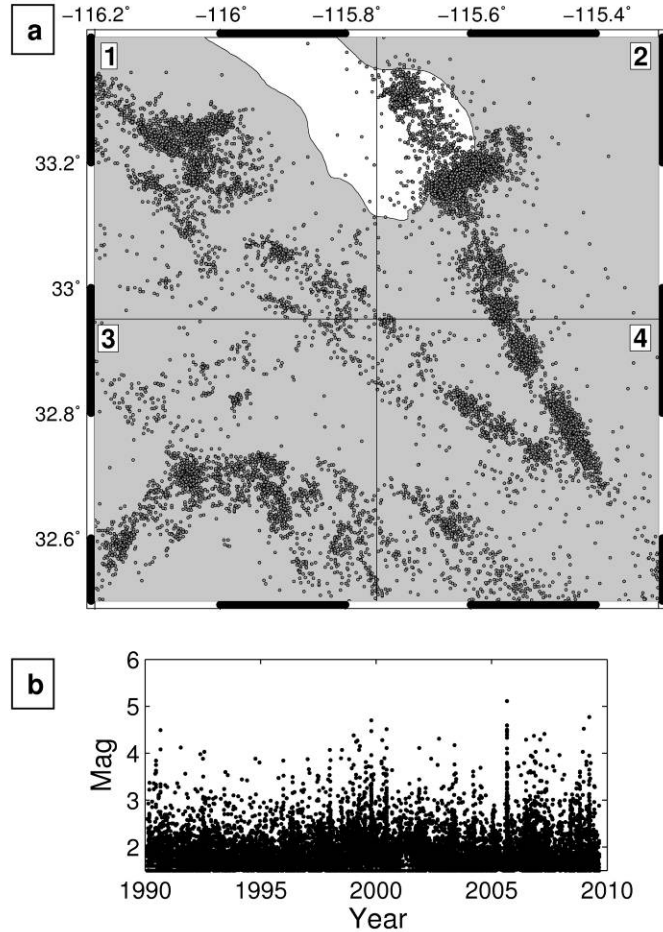


Figure 1. a) Map of the Salton Trough region in California showing $M \geq 1.5$ seismicity occurring from February 1990-August 2009, obtained from the Southern California Earthquake Data Center. For our analysis, the region is divided into the 4 boxes indicated. b) Magnitude-time history of the Salton Trough catalog.

We analyze a catalog of $M \geq 1.5$ earthquakes that occurred in the Salton Trough from February 1990 to August 2009. We choose a magnitude cutoff of 1.5 based on frequency magnitude plots of the entire data set, as well as in each spatial bin and in time windows following the largest events to ensure that the cutoff magnitude does not change over the space-time windows under consideration. We divide the region up into 4 spatial boxes (Fig. 1) and bin the occurrence times into time windows of 20 days to obtain seismicity rates in each box. This space-time window allows us to obtain enough earthquakes in each bin to resolve the background rate. Any spatial binning scheme that obeys this criterion, such as a fault-based algorithm similar to those used in stress inversions [e.g., *Hardebeck and Hauksson, 1999*], would work and can be handled using the numerical integration technique described in *Ogata [1998]*.

We first fit the space-time ETAS model to the 2005 M5.1 Obsidian Buttes earthquake to account for as much of the aftershock behavior as possible. From the

space-time ETAS estimation algorithm [Ogata and Zhuang, 2006], the MLE for the ETAS parameters are $K = 0.53$ events/day/deg², $\alpha = 0.92$, $p = 1.3$, $c = 0.01$ days, $d = 4.8e-5$ deg², $q = 2.63$, and $\eta = 0.23$. However, the data vector formed using these parameters resulted in a number of negative seismicity rate values primarily due to the estimate of p , which can lead to instabilities in the filter due to the assumption of a Gaussian error distribution. Therefore, we instead use the ordinary-time ETAS parameters ($K = 0.61$ events/day/deg², $\alpha = 0.88$, $p = 1.1$, and $c = 0.001$ days) fit to this catalog [Llenos et al., 2009].

We subtract the ETAS-predicted rate from the observed seismicity rate to form the data vector and estimate the data covariance \mathbf{R}_k . Again because of the tradeoff between the parameters τ and $A\sigma$ and our lack of sensitivity to $A\sigma$, we fix $A\sigma$ to 1 MPa. Assuming that $A = 0.01$ from laboratory observations [Dieterich, 1994], this value of $A\sigma$ is consistent with faults that fail under hydrostatic conditions at a depth of ~ 4 km, the depth at which the Obsidian Buttes swarm occurred [Chester and Higgs, 1992; Blanpied et al., 1998; Lohman and McGuire, 2007]. Fig. 2 shows the stressing rate estimates for each box, illustrating the filter's ability to detect when and in which box the largest transient in the region occurs. The largest anomaly occurs in Box 2 and is associated with a geodetically-observed shallow aseismic creep event on the Obsidian Buttes fault that triggered an earthquake swarm in 2005 [Lohman and McGuire, 2007]. The peak forward estimate of stressing rate is 0.042 ± 0.004 MPa/day and the backsmoothed estimate is 0.022 ± 0.006 MPa/day, roughly two orders of magnitude above tectonic loading.

The second largest signal also occurred in Box 2 and corresponds to the Bombay Beach earthquake swarm that occurred in March 2009. The swarm consisted of ~ 100 s of events, the largest of which was a M4.8 that occurred three days after the swarm initiated. We also identify small anomalies in Boxes 2 and 4 in May 2003 that may be related to an earthquake swarm that occurred in the Imperial fault zone (located near the boundary of the two boxes) [Roland and McGuire, 2009]. We can also associate smaller anomalies in Box 2 with earthquake swarms that occurred in the Brawley seismic zone in 1996, 1998, and 2008 [Southern California Earthquake Center, <http://www.data.scec.org/monthly/index.php>]. While we cannot rule out the possibility of fluid flow triggering these smaller swarms, other swarms in the Salton Trough exhibit migration rates of 0.1-1 km/hr which correspond to typical rupture propagation velocities of aseismic creep events [Roland and McGuire, 2009, and references therein], rather than the rates of fractions of kilometers per day associated with fluid flow [e.g., Hainzl and Ogata, 2005].

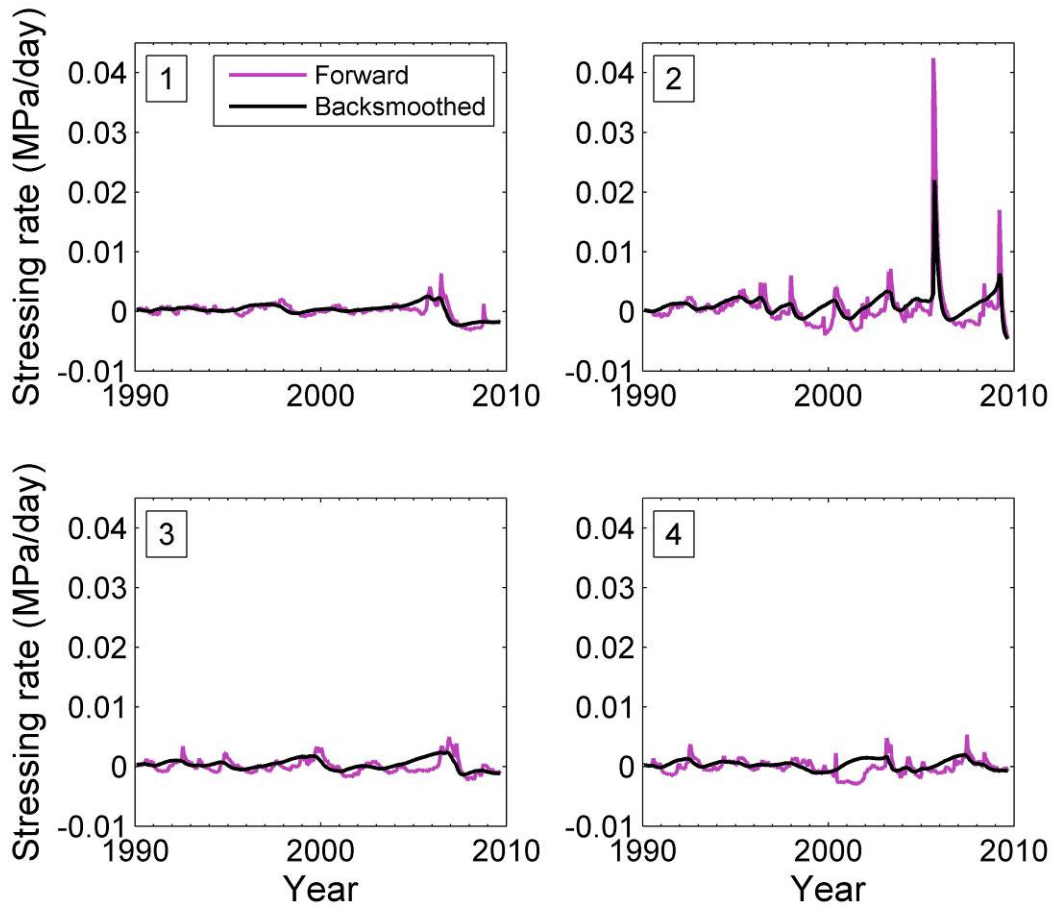


Figure 2. Filter estimates of \dot{S} in each spatial box for the Salton Trough. The purple line indicates the forward estimate, the black line indicates the backsmoothed estimate. The largest signal, in Box 2, corresponds to a geodetically-observed aseismic transient in the Obsidian Buttes in 2005 [Lohman and McGuire, 2007]. The next largest signal, also in Box 2, relates to the 2009 Bombay Beach earthquake swarm. Other smaller anomalies may be related to an earthquake swarm on the Imperial Fault in 2003 [Roland and McGuire, 2009] in Boxes 2 and 4, earthquake swarms in the Brawley seismic zone in 1996, 1998, and 2008 in Box 2, and the 2009 Bombay Beach swarm in Box 2.

Our results highlight the need for a time-dependent background seismicity rate to account for variations in seismicity rate due to aseismic processes, as other studies have suggested [e.g., Hainzl and Ogata, 2005; Lombardi et al., 2006; Lombardi and Marzocchi, 2007; Lombardi et al., 2010]. Fig. 3 compares the observed cumulative number of events in the Salton Trough catalog with the number of events predicted from optimizing the space-time ETAS model to the part of the catalog that occurred prior to the 2005 Obsidian Buttes swarm, and the number of events predicted from the filter estimate of seismicity rate. We transform the occurrence times t_i of the events in the catalog with the theoretical cumulative

function $\tau_i = \int_0^i \lambda(s) ds$, where λ is the predicted seismicity rate from either ETAS or the filter [Ogata, 1988, 2005]. A plot of the cumulative number of events vs. transformed time should be linear if the seismicity in the catalog is well described by a particular model. The 2σ error bars of the extrapolation can be calculated using $\sigma = \left[\tau - \Lambda(0, T) + \frac{\{\tau - \Lambda(0, T)\}^2}{\Lambda(0, T)} \right]^{1/2}$, based on the fact that the cumulative curves of the transformed times after $\Lambda(0, T)$ (where $\Lambda(0, T)$ is the transformed time of the last event that occurred during the time period $[0, T]$ over which the ETAS model was optimized) should behave as a standard Brownian process [Ogata, 2005]. Positive (or negative) deviations from this linear trend indicate that the model under-predicts (or over-predicts) the amount of seismicity. Fig. 3 shows that with the space-time ETAS model, a significant positive deviation from this trend occurs near the beginning of the Obsidian Buttes swarm, suggesting that anomalous seismicity is occurring that the ETAS model alone cannot explain. The filter prediction however matches the observed seismicity well. Therefore, the time-dependent background seismicity rate produced by our filter algorithm can account for the seismicity rate anomalies that appear with respect to the space-time ETAS model, which utilizes a time-independent background seismicity rate.

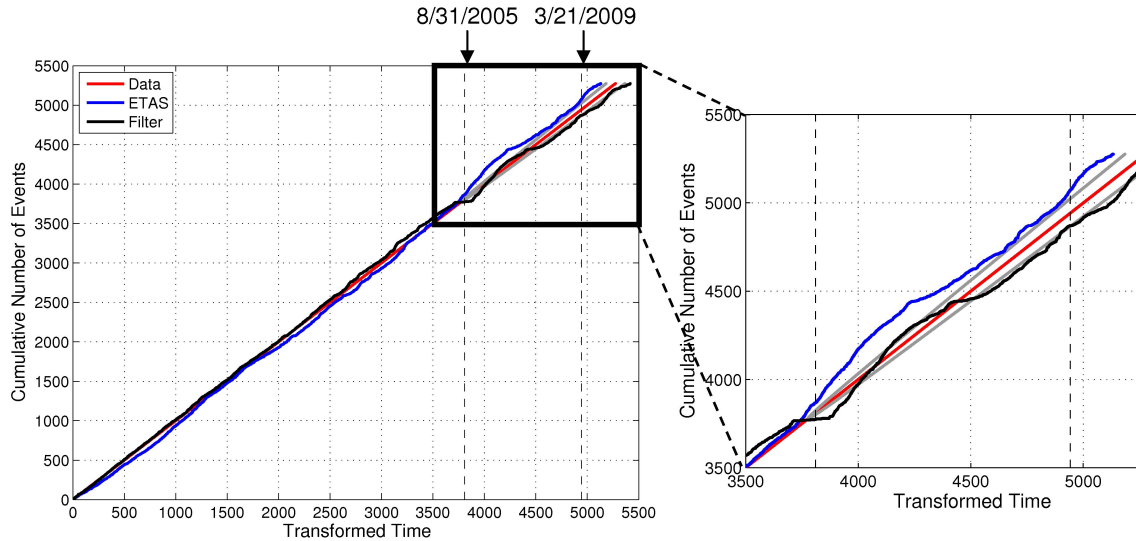


Figure 3. Cumulative number of events vs. transformed time (i.e., predicted cumulative number of events). The red line is a one-to-one line indicating a perfect fit to the observed data. ETAS transformed times are calculated with seismicity rates estimated from the space-time ETAS model optimized to just prior to the 2005 Obsidian Buttes earthquake swarm (event 3779) and extrapolated for the remainder of the catalog (blue line). Transformed times are also calculated using the filter estimate of seismicity rate (black line). The significant deviation of the blue line from the data (red line; 2σ bounds shown by gray line) shows that the ETAS model (with a time-independent background rate) under-predicts the amount of seismicity, particularly during the 2005 swarm. The filter estimate (with a time-dependent background rate) provides a better fit to the observed cumulative number of events.

To validate the estimates of stressing-rate obtained from these seismicity rate variations, we compare our peak stressing rate estimate for the 2005 Obsidian Buttes aseismic transient to an estimate based on a slip model of the deformation inverted from Interferometric Synthetic Aperture Radar (InSAR) data [Lohman and McGuire, 2007]. The seismicity triggered by this transient occurred primarily in the depth range of 4-6 km. We calculate the Coulomb stress change [King *et al.*, 1994; Lin and Stein, 2004; Toda *et al.*, 2005] at this depth range due to the aseismic slip on the shallow part of the fault and obtain an average total Coulomb stress change of 0.6 MPa (Fig. 10). Based on GPS line-length change data, the transient lasted ~ 1 -10 days [Lohman and McGuire, 2007]. Given this range of durations, the average stressing rate during the transient then becomes ~ 0.06 -0.6 MPa/day. For a duration of 5 days (which appears to best describe the GPS data), the average stressing rate is 0.12 MPa/day.

We compare this average stressing rate to our peak stressing rate estimates for the transient. We obtained a peak stressing rate of ~ 0.04 MPa/day from the forward filter estimate and a peak stressing rate of ~ 0.02 MPa/day from the

backsmoothed estimate (Fig. 2). Thus, the results from inverting the seismicity catalog are within a factor of 5 of the average stressing rate estimated from the geodetic data. Moreover, if we take the duration of the transient to match the time step in our filter (20 days) then the estimates agree extremely well (0.03 MPa/day from the stress calculation vs. 0.02-0.04 MPa/day from the filter). Given that stressing rate increases are likely to be many orders of magnitude over background plate tectonic rates [Thatcher, 2001; Toda et al., 2002; Lohman and McGuire, 2007], the Salton Trough example demonstrates the feasibility of utilizing our approach to both detect and constrain the magnitude of stressing rate transients.

The second largest anomaly in the filter stressing rate estimate (Fig. 2) is related to the 2009 Bombay Beach earthquake swarm, which began on 21 March 2009 and lasted ~1 week. The largest event was a M4.8 that occurred on 24 March 2009, three days after the swarm began. The swarm occurred on the northernmost part of a series of ladder faults offshore of Bombay Beach (Fig. 4a). Geodetic data are limited because of the fault's offshore location, but the nearest GPS station (DHLG) observed an offset at the time of the swarm. We fit daily GPS solutions from the routine Plate Boundary Observatory analyses and found a 1.0 mm offset in the east component and a -0.8 mm offset in the north component, relative to station P504 (Fig. 4b,c). To determine if the signal can be explained by the earthquake swarm or if it requires an aseismic deformation event, we constructed a simple conservative forward model of the ground deformation due to the swarm. Summing the seismic moment released during the swarm, we calculated an average focal mechanism and placed it on the northernmost ladder fault. We estimated a rupture length and width from the moment release using empirical scaling relations [Wells and Coppersmith, 1994] and assumed a shear modulus of 25 GPa. From this forward model, we obtained offsets of -0.1 mm in the east component and -0.2 mm in the north component. Our modeled displacements are factors of 10 (east component) and 4 (north component) smaller than the observed, which allows for the possibility that aseismic deformation occurred. However, the GPS data are not conclusive, and deformation was not observed in the laser strainmeter data at Durmid Hills [D. Agnew, personal comm.].

In the rate-state model, stressing rate estimates depend to an extent on the value of $A\sigma$, because this parameter controls both the instantaneous change in seismicity rate following a stress change as well as the evolution of the state variable γ [Catalli et al., 2008; Llenos et al., 2009; Cocco et al., 2010]. However, as both the synthetic test and data analysis demonstrate, our method is relatively insensitive to variations in this parameter. For the synthetic test, varying $A\sigma$ by a factor of 10 led to a change in the peak stressing rate estimate of a factor of 2. For the Salton Trough, varying this parameter by a factor of 10 led to a change in the peak stressing rate estimate of a factor of ~4. Therefore, our method can still be used to constrain relative changes in stressing rate on an order-of-magnitude scale.

Because of our lack of sensitivity to the actual value of $A\sigma$, we utilized a physically-motivated value in our Salton Trough analysis. This approach was successfully applied to detect stress changes due to a dike intrusion at Kilauea [Dieterich et al., 2000]. Using a value of $A\sigma$ consistent with hydrostatic fault

conditions at the depth at which the triggered seismicity occurred, *Dieterich et al.* [2000] obtained estimates of stress changes from the seismicity data that agreed with the stress changes calculated from geodetically-constrained boundary element models within an order of magnitude. Similarly, we do not attempt to constrain the true value of $A\sigma$ and instead choose a value consistent with local conditions, because we are primarily concerned with detecting order-of-magnitude changes in stressing rate. Our results and subsequent validation with a geodetically-derived model of deformation suggest that our method is successfully able to do so.

Lastly, it is possible that the peaks in seismicity rate observed in Box 2 are artifacts due to undetected seismicity. The ETAS estimate of background seismicity may be overestimated, particularly following large events, due to the effect of seismicity below the magnitude cutoff triggering larger events above the cutoff [*Sornette and Werner*, 2005]. However, in this case the two largest spikes that we find correspond to transient signals that were also observed on GPS (i.e., the 2005 Obsidian Buttes transient and the 2009 Bombay Beach transient). Moreover, geodetically-observed transients in other regions such as Kilauea and Boso have been shown to trigger significant changes in the ETAS-estimated background seismicity rate [*Llenos et al.*, 2009]. Finally, *Lombardi et al.* [2010] recently used simulated catalogs to demonstrate that a bias from undetected seismicity could not explain the changes in background seismicity rate observed during the 1997 Umbria-Marche earthquake sequence, which they attribute to fluid flow. Therefore, while it is possible that undetected events may cause apparent spikes in background seismicity rate, it is likely that the largest signals we detect are real variations, particularly since they correlate with GPS-detected transients.

Summary

We have developed a technique to detect aseismic transients in time and space from earthquake catalog data by combining the ETAS and rate-state models of seismicity rate into a single data assimilation algorithm to invert catalogs for stressing rate variations. We applied it to a catalog from the Salton Trough in California, and successfully detected the onset and constrained the absolute magnitude of the largest aseismic transient in a 20 year catalog to within a factor of five of the stressing rate estimated with geodetic data. We also detected an anomaly related to the 2009 Bombay Beach swarm occurring around the same time as an offset observed at a nearby GPS station, suggesting that aseismic deformation may have occurred.

Overall, the Salton Trough results suggest that our algorithm is a feasible way to detect aseismic stressing rate transients strictly from seismicity catalog data. This method may ultimately enable aseismic transient detection in regions lacking good geodetic data resolution, such as the (offshore) updip part of subduction zone faults, and in time periods prior to the widespread availability of geodetic data. Additionally, a seismicity based approach may be more sensitive to small (M4-5) and/or shallow slow-slip transients that are not detected by even dense geodetic networks such as the Plate Boundary Observatory [*Wei et al.*, 2009]. The results suggest that our seismicity inversion method provides an accurate way to detect

and locate transient deformation strictly from seismicity catalogs and can constrain the absolute magnitude of stressing rate variations.

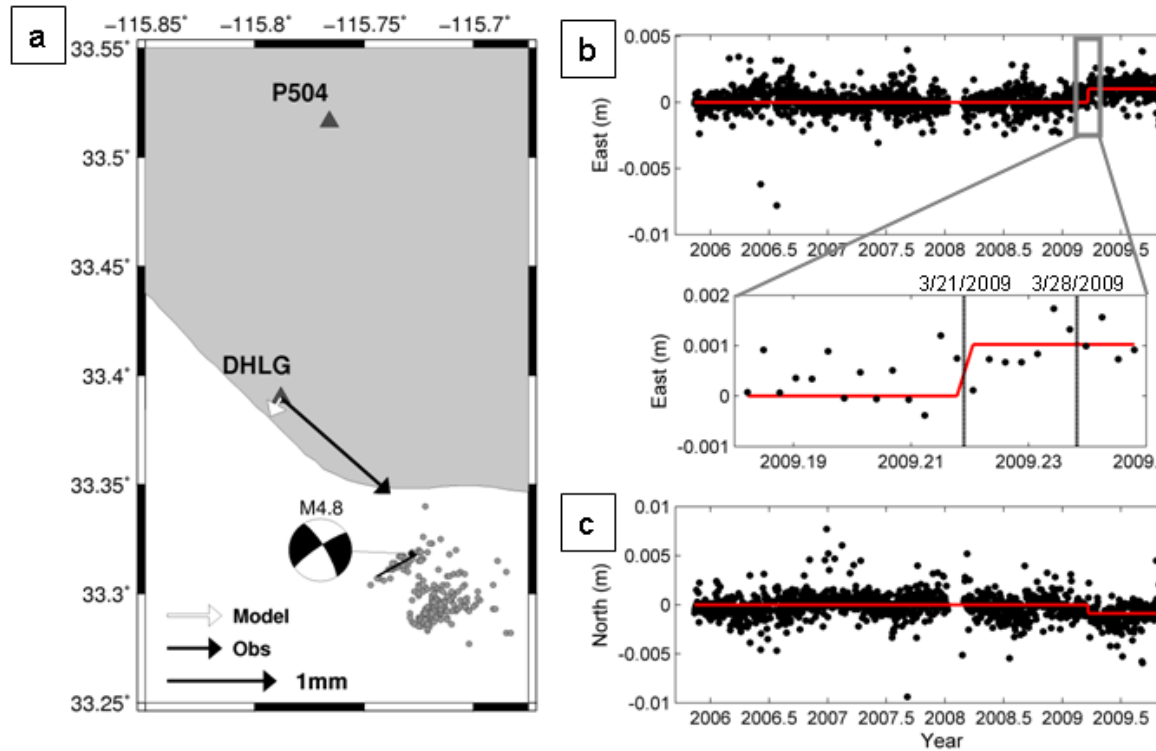


Figure 4. a) Map of the Bombay Beach region showing $M > 1.5$ seismicity during the swarm (gray dots). Vectors indicate the observed (black) and modeled (white) displacement at station DHLG relative to station P504. Displacements were modeled assuming the total moment release of the swarm occurred on the northernmost ladder fault. The focal mechanism of the M4.8 event is also shown. b) Eastward component of displacement at DHLG relative to P504, observed from daily GPS solutions from PBO analyses (black dots). Linear trend (red line) obtained by fitting the time periods before and after the swarm. An offset of ~ 1 mm occurs around the time of the swarm. c) North component of displacement at DHLG relative to P504 (black dots), with linear trend (red line) fit to before and after the swarm. An offset of 0.8mm to the south occurs around the time of the swarm.

Bibliography (Papers resulting from this grant)

Llenos, A. L, and J. J. McGuire, Detecting Aseismic Strain Transients From Seismicity Data, *J. Geophys. Res.*, in press 2011.

References

- Anderson, B. D. O., and J. B. Moore (2005), *Optimal Filtering*, Dover, Mineola, NY.
- Ben-Zion, Y., and V. Lyakhovsky (2006), Analysis of aftershocks in a lithospheric model with seismogenic zone governed by damage rheology, *Geophys. J. Int.*, *165*, 197-210, doi:10.1111/j.1365-246X.2006.02878.x.
- Blanpied, M. L., C. J. Marone, D. A. Lockner, J. D. Byerlee, and D. P. King (1998), Quantitative measure of the variation in fault rheology due to fluid-rock interactions, *J. Geophys. Res.*, *103*, 9691-9712.
- Brune, J. N., and C. R. Allen (1967), A low-stress-drop, low-magnitude earthquake with surface faulting: The Imperial, California, earthquake of March 4, 1966, *Bull. Seis. Soc. Am.*, *57*, 501-514.
- Chester, F. M., and N. G. Higgs (1992), Multimechanism friction constitutive model for ultrafine quartz gouge at hypocentral conditions, *J. Geophys. Res.*, *97*, 1859-1870.
- Daley, D. J., and D. Vere-Jones (2002), *An Introduction to the Theory of Point Processes*, vol. 1, 2nd ed., Springer-Verlag, New York.
- Delahaye, E. J., J. Townend, M. E. Reyners, and G. Rogers (2009), Microseismicity but no tremor accompanying slow slip in the Hikurangi subduction zone, New Zealand, *Earth Planet. Sci. Lett.*, *277*, 21-28, doi:10.1016/j.epsl.2008.09.038.
- Dieterich, J. (1994), A constitutive law for rate of earthquake production and its application to earthquake clustering, *J. Geophys. Res.*, *99*, 2601-2618.
- Dieterich, J., V. Cayol, and P. Okubo (2000), The use of earthquake rate changes as a stress meter at Kilauea volcano, *Nature*, *408*, 457-460.
- Enescu, B., S. Hainzl, and Y. Ben-Zion (2009), Correlations of seismicity patterns in Southern California with surface heat flow data, *Bull. Seism. Soc. Am.*, *99*, 3114-3123, doi:10.1785/0120080038.
- Felzer, K. R., T. W. Becker, R. E. Abercrombie, G. Ekström, and J. R. Rice (2002), Triggering of the 1999 M_w 7.1 Hector Mine earthquake by aftershocks of the 1992 M_w 7.3 Landers earthquake, *J. Geophys. Res.*, *107*(B9), 2190, doi:[10.1029/2001JB000911](https://doi.org/10.1029/2001JB000911).
- Fukuda, J., and K. M. Johnson (2008), A fully Bayesian inversion for spatial distribution of fault slip with objective smoothing, *Bull. Seis. Soc. Am.*, *98*, 1128-1146, doi:10.1785/0120070194.

Gelb, A. (1974), *Applied Optimal Estimation*, MIT Press, Cambridge, MA.

Hainzl, S., and Y. Ogata (2005), Detecting fluid signals in seismicity data through statistical earthquake modeling, *J. Geophys. Res.*, *110*, doi:10.1029/2004JB003247.

Hainzl, S., B. Enescu, M. Cocco, J. Woessner, F. Catalli, R. Wang, and F. Roth (2009), Aftershock modeling based on uncertain stress calculations, *J. Geophys. Res.*, *114*, B05309, doi:10.1029/2008JB006011.

Hardebeck, J. L., and E. Hauksson (1999), Role of fluids in faulting inferred from stress field signatures, *Science*, *285*, 236– 239.

Harvey, A. C. (1989), *Forecasting, Structural Time Series Models and the Kalman Filter*, Cambridge Univ Press, New York.

Helmstetter, A. (2003), Is earthquake triggering driven by small earthquakes?, *Phys. Rev. Lett.*, *91*, doi:10.1103/PhysRevLett.91.058501.

Helmstetter, A., and B. E. Shaw (2006), Relation between stress heterogeneity and aftershock rate in the rate-and-state model, *J. Geophys. Res.*, *111*, B07304, doi:10.1029/2005JB004077.

Helmstetter, A., and D. Sornette (2002), Subcritical and supercritical regimes in epidemic models of earthquake aftershocks, *J. Geophys. Res.*, *107*(B10), 2237, doi:[10.1029/2001JB001580](https://doi.org/10.1029/2001JB001580).

Helmstetter, A., and D. Sornette (2003a), Båth's law derived from the Gutenberg-Richter law and from aftershock properties, *Geophys. Res. Lett.*, *30*, doi:10.1029/2003GL018186.

Helmstetter, A., and D. Sornette (2003b), Importance of direct and indirect triggered seismicity in the ETAS model of seismicity, *Geophys. Res. Lett.*, *30*(11), 1576, doi:[10.1029/2003GL017670](https://doi.org/10.1029/2003GL017670).

Hill, D. P. (1977), A model for earthquake swarms, *J. Geophys. Res.*, *82*, 1347-1352.

Hill, D. P., P. Mowinckel, and L. G. Peake (1975), Earthquakes, active faults and geothermal areas in the Imperial Valley, California, *Science*, *188*, 1306-1308.

Johnson, C. E., and D. M. Hadley (1976), Tectonic implications of the Brawley earthquake swarm, Imperial Valley, California, January 1975, *Bull. Seis. Soc. Am.*, *66*, 1133-1144.

King, G. C. P., R. S. Stein, and J. Lin (1994), Static stress changes and the triggering of earthquakes, *Bull. Seis. Soc. Am.*, *84*, 935-953.

Kisslinger, C., and L. M. Jones (1991), Properties of aftershock sequences in southern California, *J. Geophys. Res.*, *96*, 11,947-11,958.

Lin, J. and R.S. Stein (2004), Stress triggering in thrust and subduction earthquakes, and stress interaction between the southern San Andreas and nearby thrust and strike-slip faults, *J. Geophys. Res.*, *109*, B02303, doi:[10.1029/2003JB002607](https://doi.org/10.1029/2003JB002607).

Llenos, A. L., J. J. McGuire, and Y. Ogata (2009), Modeling seismic swarms triggered by aseismic transients, *Earth Planet. Sci. Lett.*, *281*, 59-69, doi:10.1016/j.epsl.2009.02.011.

Lohman, R. B., and J. J. McGuire (2007), Earthquake swarms driven by aseismic creep in the Salton Trough, California, *J. Geophys. Res.*, *112*, B04405, doi:10.1029/2006JB004596.

Lombardi, A. M., and W. Marzocchi (2007), Evidence of clustering and nonstationarity in the time distribution of large worldwide earthquakes, *J. Geophys. Res.*, *112*, B02303, doi:10.1029/2006JB004568.

Lombardi, A. M., W. Marzocchi, and J. Selva (2006), Exploring the evolution of a volcanic seismic swarm: The case of the 2000 Izu Islands swarm, *Geophys. Res. Lett.*, *33*, L07310, doi:10.1029/2005GL025157.

Lombardi, A. M., M. Cocco, and W. Marzocchi (2010), On the increase of background seismicity rate during the 1997-1998 Umbria-Marche, Central Italy, Sequence: Apparent variation or fluid-driven triggering?, *Bull. Seism. Soc. Am.*, *100*, 1138-1152, doi:10.1785/0120090077.

Marsan, D. (2006), Can coseismic stress variability suppress seismicity shadows? Insights from a rate-and-state friction model, *J. Geophys. Res.*, *111*, B06305, doi:10.1029/2005JB004060.

McGuire, J. J., and P. Segall (2003), Imaging of aseismic fault slip transients recorded by dense geodetic networks, *Geophys. J. Int.*, *155*, 778-788.

McGuire, J. J., M. S. Boettcher, and T. H. Jordan (2005), Foreshock sequences and short-term earthquake predictability on East Pacific Rise transform faults, *Nature*, *434*, doi:10.1038/nature03377.

Montgomery-Brown, E. K., P. Segall, and A. Miklius (2009), Kilauea slow slip events: Identification, source inversions, and relation to seismicity, *J. Geophys. Res.*, *114*, B00A03, doi:10.1029/2008JB006074.

Ogata, Y. (1988), Statistical models for earthquake occurrences and residual analysis for point processes, *J. Am. Stat. Assoc.*, *83*, 9-27.

- Ogata, Y. (1998), Space-time point process models for earthquake occurrences, *Ann. Inst. Statist. Math.*, 50, 379-402.
- Ogata, Y. (2004), Space-time model for regional seismicity and detection of crustal stress changes, *J. Geophys. Res.*, 109, B03308, doi:10.1029/2003JB002621.
- Ogata, Y. (2005), Detection of anomalous seismicity as stress change sensor, *J. Geophys. Res.*, 110, B05S06, doi:10.1029/2004JB003245.
- Ogata, Y., and J. Zhuang (2006), Space-time ETAS models and an improved extension, *Tectonophysics*, 413, doi:10.1016/j.tecto.2005.10.016.
- Omori, F. (1894), On the aftershocks of earthquakes, *J. Coll. Sci. Imp. Univ. Tokyo*, 7, 111-200.
- Ozawa, S., H. Suito, and M. Tobita (2007), Occurrence of quasi-periodic slow-slip off the east coast of the Boso peninsula, Central Japan, *Earth Planets Space*, 59, 1241-1245.
- Richter, C. F. (1958), *Elementary Seismology*, W. H. Freeman, San Francisco.
- Roland, E., and J. J. McGuire (2009), Earthquake swarms on transform faults, *Geophys. J. Int.*, 178, 1677-1690, doi:10.1111/j.1365-246X.2009.04214.x.
- Rubin, A. M., and D. Gillard (2000), Aftershock asymmetry/rupture directivity among central San Andreas fault microearthquakes, *J. Geophys. Res.*, 105(B8), 19, 095-19, 109.
- Segall, P., and M. Matthews (1997), Time dependent inversion of geodetic data, *J. Geophys. Res.*, 102, 22,391-22,409.
- Segall, P., E. K. Desmarais, D. Shelly, A. Miklius, and P. Cervelli (2006), Earthquakes triggered by silent slip events on Kilauea volcano, Hawaii, *Nature*, 442, doi:10.1038/nature04938.
- Thatcher, W. (2001), Silent slip on the Cascadia subduction interface, *Science*, 292, doi:10.1126/science.1061770.
- Toda, S., R. S. Stein, and T. Sagiya (2002), Evidence from the AD 2000 Izu islands earthquake swarm that stressing rate governs seismicity, *Nature*, 419, 58-61.
- Toda, S., R. S. Stein, K. Richards-Dinger and S. Bozkurt (2005), Forecasting the evolution of seismicity in southern California: Animations built on earthquake stress transfer, *J. Geophys. Res.*, 110, B05S16, doi:[10.1029/2004JB003415](https://doi.org/10.1029/2004JB003415).

Utsu, T. (1961), A statistical study on the occurrence of aftershocks, *Geophys. Mag.*, *30*, 521-605.

Wei, M., D. Sandwell, and Y. Fialko (2009), A silent M_w 4.7 slip event of October 2006 on the Superstition Hills fault, southern California, *J. Geophys. Res.*, *114*, B07402, doi:10.1029/2008JB006135.

Wells, D. L., and K. J. Coppersmith (1994), New empirical relationships among magnitude, rupture length, rupture width, rupture area, and surface displacement, *Bull. Seis. Soc. Am.*, *84*, 974-1002.

Wessel, P., and W. H. F. Smith (1998), New, improved version of generic mapping tools released, *Eos Trans. AGU*, *79*(47), 579

Werner, M. J. (2008), On the fluctuations of seismicity and uncertainties in earthquake catalogs: Implications and methods for hypothesis testing, Ph.D. thesis, 308 pp., Univ. of Calif. Los Angeles, Los Angeles.

Werner, M. J., K. Ide, and D. Sornette (2009), Earthquake forecasting based on data assimilation: Sequential Monte Carlo methods for renewal processes, arXiv:0908.1516 [physics.geo-ph].

Williams, P. L., and H. W. Magistrale (1989), Slip along the Superstition Hills fault associated with the 24 November 1987 Superstition Hills, California, earthquake, *Bull. Seis. Soc. Am.*, *79*, 390-410.

Wolfe, C. J., B. A. Brooks, J. H. Foster, and P. G. Okubo (2007), Microearthquake streaks and seismicity triggered by slow earthquakes on the mobile south flank of Kilauea Volcano, Hawai'i, *Geophys. Res. Lett.*, *34*, L23306, doi:10.1029/2007GL031625.

Yang, W., and Y. Ben-Zion (2009), Observational analysis of correlations between aftershock productivities and regional conditions in the context of a damage rheology model, *Geophys. J. Int.*, *177*, 481-490.

Zhuang, J., C.-P. Chang, Y. Ogata, and Y.-I. Chen (2005), A study on the background and clustering seismicity in the Taiwan region by using point process models, *J. Geophys. Res.*, *110*, B05S18, doi:10.1029/2004JB003157.